processes

MDPI

Article

Chromium VI and Fluoride Competitive Adsorption on Different Soils and By-Products

Ana Quintáns-Fondo [1], Gustavo Ferreira-Coelho [1], Manuel Arias-Estévez [2], Juan Carlos Nóvoa-Muñoz [2], David Fernández-Calviño [2], Esperanza Álvarez-Rodríguez [1], María J. Fernández-Sanjurjo [1] and Avelino Núñez-Delgado [1,*]

1 Department of Soil Science and Agricultural Chemistry, Engineering Polytechnic School, Universidade de Santiago de Compostela, 27002 Lugo, Spain; anaquintansfondo@hotmail.com (A.Q.-F.); gf_coelho@yahoo.com.br (G.F.-C.); esperanza.alvarez@usc.es (E.Á.-R.); mf.sanjurjo@usc.es (M.J.F.-S.)

2 Department of Plant Biology and Soil Science, Faculty of Sciences, Campus Ourense, Universidade de Vigo, 32004 Ourense, Spain; mastevez@uvigo.es (M.A.-E.); edjuanca@uvigo.es (J.C.N.-M.); davidfc@uvigo.es (D.F.-C.)

* Correspondence: avelino.nunez@usc.es; Tel.: +34-982-823-140

Received: 24 September 2019; Accepted: 12 October 2019; Published: 15 October 2019

Abstract: Chromium (as Cr(VI)) and fluoride (F^-) are frequently found in effluents from different industrial activities. In cases where these effluents reach soil, it can play an important role in retaining those pollutants. Similarly, different byproducts could act as bio-adsorbents to directly treat polluted waters or to enhance the purging potential of soil. In this work, we used batch-type experiments to study competitive Cr(VI) and F^- adsorption in two different soils and several kinds of byproducts. Both soils, as well as mussel shell, oak ash, and hemp waste showed higher adsorption for F^-, while pyritic material, pine bark, and sawdust had a higher affinity for Cr(VI). Considering the binary competitive system, a clear competition between both elements in anionic form is shown, with decreases in adsorption of up to 90% for Cr(VI), and of up to 30% for F^-. Adsorption results showed better fitting to Freundlich's than to Langmuir's model. None of the individual soils or byproducts were able to adsorbing high percentages of both pollutants simultaneously, but it could be highly improved by adding pine bark to increase Cr(VI) adsorption in soils, thus drastically reducing the risks of pollution and deleterious effects on the environment and on public health.

Keywords: adsorption; chromium; competition; fluoride; soil and water pollution

1. Introduction

In recent years there has been growing concern regarding F^- and Cr(VI) pollution, due to both substances being transported into effluents from industries related to the extraction of minerals, foundries, dyes and pigments, semiconductors, and glass manufacturing [1,2]. These effluents can reach surface- and ground-waters by direct discharge or after passing through soils. Authors such as Rafique et al. [3] or Kumar et al. [4] indicate that there is a global hazard as regards fluoride and chromium pollution, taking into account that their permissible limits in drinking water (1.5 and 0.05 mg L^{-1}, respectively, as per the World Health Organization) are widely exceeded in occasions, some of them referenced for countries such as India, China, USA, Mexico, or Argentina.

A F^- concentration between 0.5–1.0 mg L^{-1} in drinking water can be considered beneficial for bones and teeth, but it can cause fluorosis and even neurological damage when it is higher than 1.5 mg L^{-1} [5]. In the case of Cr, although Cr(III) is indispensable in low quantities, Cr(VI) is considered highly toxic due to its mutagenic, carcinogenic, and teratogenic potential [6]. Given that it is extremely improbable that a ban will be implemented in the short term in order to remove F^- and Cr(VI) from

industrial use (mainly in aluminum, textile, or leather tanning factories), it is of main importance to determine the capacity of soils to retain both anions, aiding to prevent their entry into waterbodies and plant uptake, as well as to develop low-cost methodologies to increase soil retention capacity and to remove these toxics when they reach waters [4].

Although different methodologies have been developed to remove F^- and Cr(VI) from waters, such as precipitation, electrocoagulation, ion exchange, or electro-dialysis, the use of adsorbent materials has been considered as the most economical and sustainable alternative [2]. Previous works have dealt with individual adsorption of F^- and Cr(VI), separately, both in soils and in different waste materials [3,7–13]. In addition, some studies focused on simultaneous retention of F^- and Cr(VI), using adsorbents such as a chitosan-alginate aluminum complex (CSAlg-Al) [4], or synthetic mesoporous alumina [2]. However, there is not enough information on simultaneous retention of these two anions in different soils, as well as on the adsorbent capacity of different byproducts derived from industrial activities.

Galicia (NW Spain) is one of the geographical areas affected by activities which cause environmental pollution by F^- and Cr(VI) (mining, aluminum factories, glass, dyes, leather tanning), and where it is also easy to obtain locally different by-products that could be used as low-cost sorbents for both pollutants [10–13]. Taking into account this previous background, the objectives of this work are: (1) to determine the capacity of forest and vineyard soils to adsorb F^- and Cr(VI) simultaneously; (2) to determine the adsorption capacity for both anions of byproducts from forestry (oak ash, pine bark, and pine sawdust), from agriculture (hemp waste), from mining (pyritic material), and from the food industry (mussel shell). The results of this study could aid to solve environmental issues due to both pollutants in waters and soils, and at the same time promote the productive recycling of by-products.

2. Materials and Methods

2.1. Materials

In Galicia (NW Spain), some environmental problems related to F^- and Cr(VI) pollution have been previously pointed out [10–13]. In fact, the soils and sorbent materials used in this work to study F^- and Cr(VI) competitive adsorption were the same previously described when performing individual adsorption tests for these two anions [13], in addition to pine sawdust, also previously described [12]. Specifically, in the current work we used samples of forest and vineyard soils, pyritic material, fine mussel shell, pine bark, oak ash, hemp waste, and pine sawdust. Taking into account that detailed descriptions for all these materials were previously published in the referred works, data on it are included in Supplementary Material. In fact, specific references regarding Supplementary Material are also included [14–37].

2.2. Methods

2.2.1. Characterization of the Soil Samples and Sorbent Materials

Details on all methods used to characterize soils and by-products, as well as the results of those procedures, are shown in Supplementary Material. Specifically, total C and N contents, pH in distilled water, pH of the point of zero charge (pH_{pzc}), exchangeable Na, K, Ca, Mg, and Al, effective cation exchange capacity (eCEC), total P, total concentrations of Na, K, Ca, Mg, Al, Fe, Mn, As, Cd, Cr, Cu, Ni, Pb, and Zn, non-crystalline Al and Fe (Al_o, Fe_o), and particle-size distribution for forest and vineyard soils. Also, infrared spectroscopy was used to determine the main functional groups present in each soil and byproduct.

2.2.2. Competitive Adsorption Experiments for F^- and Cr(VI)

A methodology similar to that previously described by Romar-Gasalla et al. [13] was used for these experiments. Specifically, each of the individual samples of soils and by-products were added with F^- and Cr(VI) simultaneously. To do that, 3 g of each sample were stirred with 30 mL of a 0.01 M

$NaNO_3$ solution in which F^- and Cr(VI) were incorporated at the same concentration (0.5, 1.5, 3, and 6 mmol L^{-1} of each anion), using analytical grade KF (Panreac, Spain) and $K_2Cr_2O_7$ (Panreac, Spain). All these suspensions were stirred for 24 h, centrifuged for 15 min (6167× g), and filtered by acid washed paper (Whatman, Spain). ICP Mass (Varian 820-NS, USA) was used to determine Cr(VI) concentration in the filtrated liquid, and F^- was quantified by means of an ion-selective electrode and TISAB IV (Orion Research, Cambridge, MA, USA). Triplicate determinations were carried out in all cases.

The amounts of F^- and Cr(VI) adsorbed were calculated as the difference between those added and those remaining in solution at equilibrium.

2.2.3. Modeling Adsorption

Adsorption data were firstly adjusted to the Langmuir and Freundlich models. The Langmuir model corresponds to the following equation:

$$Q_{eq} = \frac{Q_{max} \times K_L \times C_e}{(1 + K_L \times C_e)} \quad (1)$$

where Qeq is the amount of F^- or Cr(VI) adsorbed (mmol kg^{-1}), K_L is the Langmuir's constant related to the adsorption energy ((L $mmol^{-1}$), C_e is the concentration of F^- or Cr(VI) in the equilibrium solution (mmol L^{-1}), and Q_{max} is the maximum adsorption capacity (mmol kg^{-1}).

The Freundlich model (Equation (2)) corresponds to the equation:

$$Q_{eq} = K_F \times C_e^{1/n} \quad (2)$$

where K_F is the Freundlich's constant related to the adsorption energy (L^n kg^{-1} $mmol^{(1-n)}$), and n is the constant related to the adsorption intensity (dimensionless).

In a second step, adsorption data was adjusted to the Tempkin model (Equation (3)):

$$q_a = \beta \ln K_T + \beta \ln C_e \quad (3)$$

where $\beta = RT/b_t$ and b_t is the Temkin isotherm constant; K_t is the Tempkin isotherm equilibrium binding constant (L g^{-1}); T is Temperature (25 °C) (K = 298°), and R is the universal gas constant (8314 Pa m^3/mol K).

3. Results and Discussion

3.1. F^- and Cr(VI) Competitive Adsorption in a Binary System

Figure 1 shows F^- and Cr(VI) adsorption in a competitive (binary) system, as well as data corresponding to an individual (simple) system (from Romar-Gasalla et al. [13]).

In the binary competitive system, two kinds of behavior can be observed. On the one hand, both soils, mussel shell, oak ash, and hemp waste present higher adsorption for F^- (between 15 and 42 mmol kg^{-1}) than for Cr(VI) (between 8 and 19 mmol kg^{-1}) for the highest concentrations added (Figure 1), which becomes more evident when results are expressed as percentages (25–70% for F^-, and 1–30% for Cr (VI)). On the other hand, pine bark, sawdust and, in general, pyritic material, have a higher affinity for Cr(VI) (39–60 mmol kg^{-1}, representing between 22–99% of the highest concentration added) than for F^- (1.5–11 mmol kg^{-1}, representing 1–67% of the highest concentration added) (Figure 1). In the previous study, carried out in individual (simple) systems for Cr(VI) and F^- separately (Romar-Gasalla et al. [13]), the highest F^- adsorption corresponded to forest soil, pyritic material, pine bark, and oak ash, with values between 30 and 40 mmol kg^{-1}, which represented between 60–72% of the highest concentration of F^- added, while pine bark, pine sawdust, and pyritic material showed the highest adsorption of Cr(VI) for the highest concentration of Cr(VI) added, with

69, 40, and 32 mmol kg^{-1}, representing 98, 68, and 55%, respectively. Li et al. [2] found higher affinity for F^- than for Cr(VI) in synthetic alumina gels, while Mohapatra et al. [38] obtained the opposite result in alumina nanofibers.

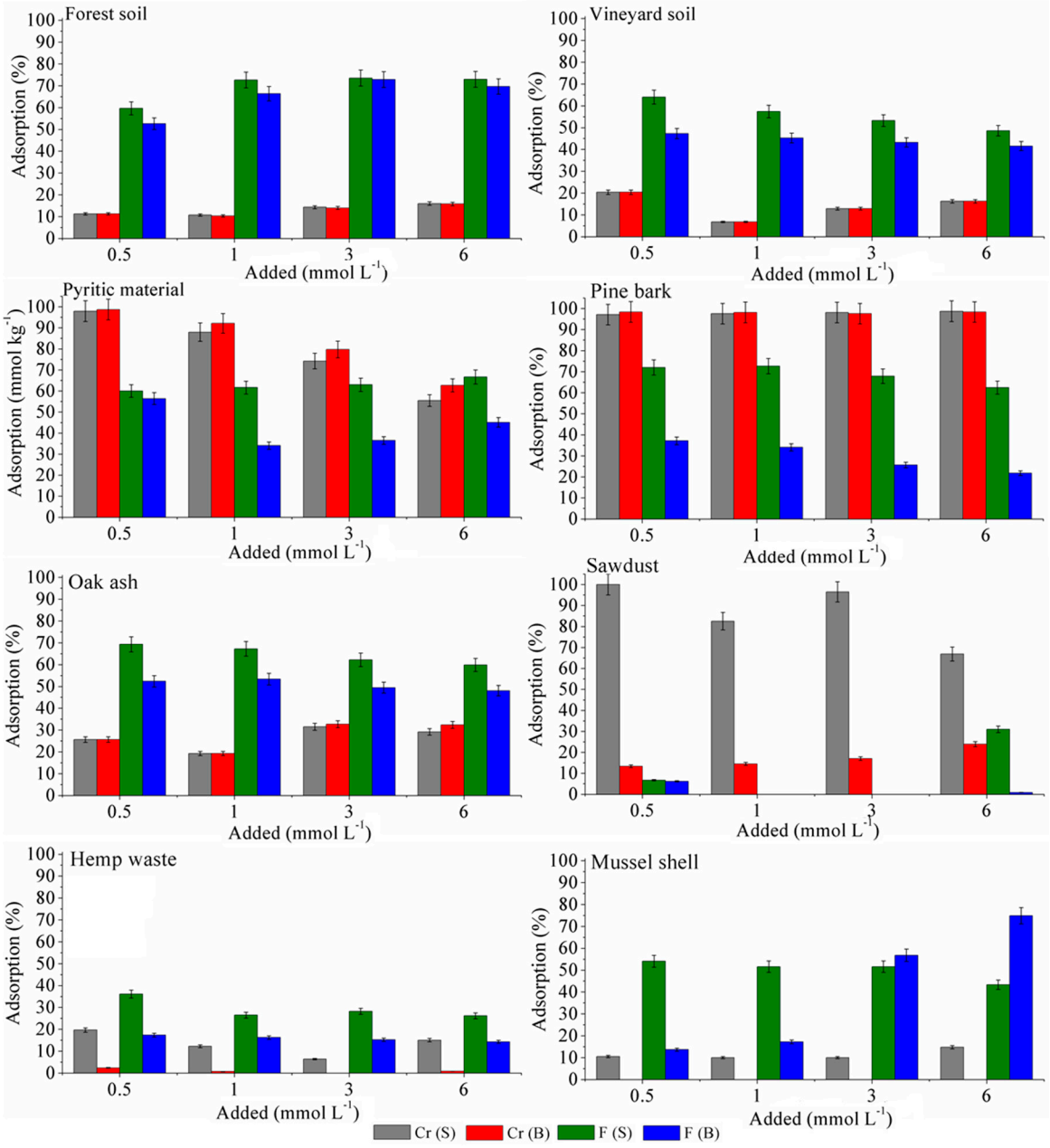

Figure 1. Percentage adsorption for Cr(VI) and F^- in the various soils and sorbents tested, in simple (S) and binary (B) systems. Average values for three replicates, with error bars showing that coefficients of variation were <5%.

The behavior observed in the present study can be related to the different composition of the sorbent materials used, and to their pH values (Table S1, Supplementary Material). Specifically, those sorbents having more acidic pH (pine bark, sawdust, and pyritic material) show higher adsorption for Cr(VI) than for F^-, because Cr(VI) adsorption is higher in clearly acid media, decreasing in alkaline and slightly acidic conditions [39,40], as the $HCrO_4^-$ species, present in acid media, is more intensively adsorbed than CrO_4^{2-}, which predominates in alkaline conditions [41].

In the case of pine bark and sawdust, acidic conditions favor the protonation of the phenolic groups present in organic compounds [42,43], electrostatically attracting negatively charged Cr(VI) species. In the case of the pyritic material, the positive charges of non-crystalline Fe minerals favor Cr(VI) adsorption, as observed in previous studies [44,45]. However, when the materials have a high concentration of non-crystalline Al minerals, such as in forest soil, vineyard soil, and oak ash (Table S1, Supplementary Material), the affinity for F^- is very high, as previously pointed out [10,11,46]. In the case of mussel shell, high F^- adsorption may be related to binding to the surface of carbonates through inner-sphere complexes with octahedral Ca [11,47].

Comparing percentage adsorption in binary and simple systems (Figure 1), it is clear that in the binary system F^- interferes Cr(VI) retention in sawdust, hemp waste, and mussel shell, decreasing Cr(VI) adsorption up to 90, 20, and 12%, respectively. Likewise, Cr(VI) decreases F^- adsorption in the binary system up to 30% in the pyritic material and pine bark, up to 12% in hemp waste and vineyard soil, and less than 10% in forest soil.

Li et al. [2] found for synthetic alumina gels that the coexistence of F^- and Cr(VI) in solution decreased Cr(VI) adsorption, but enhanced F^- adsorption, due to the fact that alumina has higher affinity for F^- than for Cr(VI), and Cr can form $\equiv CrOH_2^+$ groups, which could be new adsorption sites for F^-.

Deng et al. [48], studying competitive adsorption in fibers impregnated with cerium, found that F^- adsorption increased in a binary system in relation to a simple system, whereas Cr(VI) adsorption decreased (i.e., Cr(VI) favored F^- adsorption, but F^- hindered Cr(VI) adsorption). In addition, Wu et al. [49] reported that Cr(VI) enhanced the adsorption of another anion (anionic As) on activated carbon in a binary system.

In the present study, Cr(VI) hinders F^- adsorption (except in mussel shell for the highest concentrations of both pollutants), and F^- decreases Cr(VI) adsorption in sawdust, hemp waste, and mussel shell (Figure 1), and overall results indicate that Cr(VI) and F^- compete for adsorption sites. The decrease in the adsorption of each anion in the binary system (in relation to the simple system) can be related to the fact that F^- and some of the Cr(VI) species ($HCrO_4^-$, $Cr_2O_7^{2-}$, CrO_4^{2-}) have similar mechanisms of adsorption, and compete with each other [2]. Liu et al. [50], studying competitive adsorption between F^- and As(V) in Fe, Al, and Fe and Al oxyhydroxides, found that Fe oxyhydroxides have a high capacity to adsorb another element in anionic form (As(V)), but very little to adsorb F^-, while Al oxyhydroxides (AlO_xH_y) have a high capacity to adsorb both anions, but the efficiency depends on pH value, and there is an important competition between both anions for adsorption sites; and, finally, the mixed oxyhydroxides $FeAlO_xH_y$ have a high capacity to adsorb F^- and As(V) over a wide range of pH, and no competition was observed.

Taking into account that in the forest soil there is a lower decrease of Cr(VI) and F^- adsorption in the binary system as compared to the simple system, it would indicate absence of competition between F^- and Cr(VI) for adsorption sites in that soil, which could be due to its high concentrations of Fe and Al oxyhydroxides (Table S1, Supplementary Material), with a high capacity to adsorb F^- and Cr(VI) without competition at the concentrations tested (up to 6 mmol L^{-1} for each one). However, it must be noted that none of the materials here studied show a high capacity to adsorb simultaneously both pollutants.

Overall, in cases of contamination where both pollutants are present simultaneously, the forest soil would be able to retain up to 70% of F^- (Figure 1), but the incorporation of pine bark would be needed to also adsorb high percentages of Cr(VI). Regarding the vineyard soil, the incorporation of pine bark would increase Cr(VI) and F^- adsorption up to 94% and 86%, respectively, while oak ash could increase F^- adsorption up to 74%, as shown in a previous study [13].

3.2. Fitting to Adsorption Models

Table 1 shows fitting of adsorption data to the Langmuir model for F^- and Cr(VI) in binary and simple systems, while Table 2 presents fitting to the Freundlich model.

As shown in this Table, the existence of high errors prevents valid adjustments to the Langmuir model in most sorbents. In the case of Cr(VI), R^2 values corresponding to the Langmuir model are higher than 0.9 for the two sorbents, which are adjustable. Table 2 shows that in the Freundlich model R^2 values are higher than 0.93, except for hemp waste. Therefore, Cr(VI) adsorption is better adjusted to the Freundlich's equation, coinciding with what was pointed out by other authors [13,44,45,51,52]. In the case of F^-, R^2 values are generally high for both models (in those sorbents which are adjustable), as found in previous studies [10,13,46], but in the current work there are several sorbents for which the errors associated to parameters in the Langmuir equation are also too high, preventing from valid adjustments being made in these cases.

Table 1 also shows that in the materials for which the adjustment of F^- adsorption to Langmuir is good, Q_{max} (maximum adsorption capacity) is higher in the simple than in the binary system, coinciding with that reported by Li et al. [2], which would indicate a competition between F^- and Cr(VI) for the adsorption sites in these materials. The K_L parameter is related to the energy of adsorption [53], and in the present study it is generally higher in the binary than in the simple system (Table 1), indicating that this anion occupies the places of higher binding energy, even though F^- adsorption is smaller in the binary than in the simple system. In addition, in the binary system, K_L values for F^- correlated significantly with non-crystalline Al ($r = 0.63$, $p < 0.01$), and also with cation exchange capacity ($r = 0.75$, $p < 0.05$).

Table 1. Parameters of the Langmuir model for Cr(VI) and F^- in individual simple (S) and competitive binary (B) systems.

Adsorbent	Adsorbate	Langmuir Parameters				
		Q_{max} (mmol kg^{-1})	Error	K_L (L mmol^{-1})	Error	R^2
Forest soil	Cr (S)	-	-	-	-	-
	Cr (B)	-	-	-	-	-
	F (S)	-	-	-	-	-
	F (B)	-	-	-	-	-
Vineyard soil	Cr (S)	-	-	-	-	-
	Cr (B)	-	-	-	-	-
	F (S)	82.050	9.960	0.188	0.030	0.999
	F (B)	43.418	10.653	0.407	0.188	0.959
Pyritic material	Cr (S)	36.594	4.049	2.636	1.012	0.970
	Cr (B)	40.779	5.260	3.320	1.540	0.947
	F (S)	-	-	-	-	-
	F (B)	-	-	-	-	-
Pine bark	Cr (S)	-	-	-	-	-
	Cr (B)	-	-	-	-	-
	F (S)	93.130	12.790	0.297	0.061	0.997
	F (B)	24.991	4.055	0.225	0.063	0.989
Hemp waste	Cr (S)	-	-	-	-	-
	Cr (B)	-	-	-	-	-
	F (S)	107.829	57.080	0.038	0.023	0.997
	F (B)	-	-	-	-	-
Pine sawdust	Cr (S)	-	-	-	-	-
	Cr (B)	-	-	-	-	-
	F (S)	31.90557	4.480	0.345	0.151	0.932
	F (B)	-	-	-	-	-
Mussel shell	Cr (S)	-	-	-	-	-
	Cr (B)	-	-	-	-	-
	F (S)	37.900	3.170	0.420	0.020	0.997
	F (B)	-	-	-	-	-
Oak ash	Cr (S)	-	-	-	-	-
	Cr (B)	26.756	2.752	0.287	0.055	0.994
	F (S)	139.780	37.080	0.140	0.050	0.997
	F (B)	5.808	0.551	0.648	0.074	0.980

Q_{max}: maximum adsorption capacity; K_L: parameter related to the strength of interaction adsorbent/adsorbate; R^2: coefficient of determination; -: error values too high for fitting.

Regarding the Freundlich model, K_F is a main parameter for which higher values are indicative of higher adsorption capacity of the adsorbents [54,55]. Overall, and contrary to that reported by Li et al. [2] for synthetic alumina gels, in the present study K_F values were lower for both anions in the binary than in the simple system (Table 2), which indicates a reduction in adsorption capacity in the binary in relation to the simple system. However, both soils, pine bark, and oak ash did not evidence variation in Cr(VI) adsorption in the presence of F^- (Figure 1). In addition, in the binary system, K_F values (and therefore adsorption capacities) were higher for F^- than for Cr(VI) in both soils, hemp waste, pine sawdust, mussel shell, and oak ash, whereas K_F was much higher for Cr(VI) in the pyritic material and in pine bark.

Table 2. Parameters of the Freundlich model for Cr(VI) and F^- in individual simple (S) and competitive binary (B) systems.

Adsorbent	Adsorbate	Freundlich Parameters				
		K_F (L^n kg^{-1} $mmol^{(1-n)}$)	Error	n	Error	R^2
Forest soil	Cr (S)	1.380	0.260	1.200	0.130	0.990
	Cr (B)	1.303	0.246	1.224	0.125	0.986
	F (S)	26.370	1.260	1.075	0.009	0.999
	F (B)	22.988	1.642	1.026	0.123	0.977
Vineyard soil	Cr (S)	0.890	0.249	1.482	0.182	0.990
	Cr (B)	0.815	0.394	1.349	0.309	0.936
	F (S)	12.180	0.250	0.778	0.002	0.999
	F (B)	11.660	1.737	0.639	0.138	0.926
Pyritic material	Cr (S)	23.343	1.171	0.381	0.045	0.980
	Cr (B)	28.504	0.075	0.344	0.002	0.999
	F (S)	17.240	0.3929	1.208	0.003	0.998
	F (B)	4.584	0.974	1.480	0.191	0.980
Pine bark	Cr (S)	8436.359	3298.200	1.976	0.153	1.000
	Cr (B)	1357.763	1269.334	1.385	0.387	0.941
	F (S)	20.238	0.837	0.771	0.005	0.994
	F (B)	4.675	0.233	0.662	0.038	0.995
Hemp waste	Cr (S)	1.515	0.263	1.094	0.109	0.993
	Cr (B)	0.059	0.053	2.037	0.889	0.876
	F (S)	4.073	0.260	0.910	0.005	0.997
	F (B)	2.875	0.612	0.687	0.145	0.968
Pine sawdust	Cr (S)	10.010	0.000	-	-	1.000
	Cr (B)	1.257	0.149	1.599	0.082	0.997
	F (S)	4.073	0.253	0.908	0.047	0.996
	F (B)	2.875	0.612	0.687	0.145	0.968
Mussel shell	Cr (S)	0.2817	0.1362	2.117	0.301	0.990
	Cr (B)	-	-	9.341	0.892	0.999
	F (S)	10.34	1.260	0.562	0.083	0.971
	F (B)	1.215	0.922	8.843	1.896	0.947
Oak ash	Cr (S)	3.536	0.766	1.112	0.163	0.980
	Cr (B)	5.808	0.551	0.648	0.074	0.980
	F (S)	17.11	0.480	0.842	0.035	0.999
	F (B)	10.585	0.216	10.585	0.020	0.999

K_F: parameter related to adsorption capacity; n: parameter related to the heterogeneity of the sorbent; R^2: coefficient of determination; -: error values too high for fitting.

The Freundlich's n parameter is related to the affinity between the adsorbent and the adsorbate (lower n values indicate higher affinity) [55], informing on the reactivity and heterogeneity of the active sites of the adsorbent. If $n = 1$, the adsorption is linear, while if $n > 1$, the adsorption is chemical, and values of $n < 1$ are indicative of high-energy heterogeneous sites, with strong interactions between molecules of adsorbate, where physical adsorption will be the most favorable, and high-energy sites are the first to be occupied [53,56,57]. Table 2 shows that n is >1 for Cr(VI) in most cases (except for

oak ash in the binary system, and for the pyritic material in both binary and simple systems), which would indicate that Cr(VI) adsorption is mainly chemical in both soils and most of the other sorbents studied, while it is mainly physical in oak ash and the pyritic material. For Cr(VI), the *n* parameter presents very similar values for binary and simple systems in both soils and in the pyritic material, whereas *n* decreases in the binary system for pine bark and oak ash, and increases for pine sawdust, mussel shell, and hemp waste. Therefore, the presence of F^- generally modifies Cr(VI) affinity for the sorbents (except for both soils and the pyritic material), increasing affinity for pine bark and oak ash, and decreasing it for mussel shell, hemp waste, and pine sawdust.

This was confirmed in practice by the adsorption experiments (Figure 1), with the exception of pine bark and mussel shell, which had a high affinity for Cr(VI) not further affected by the presence of F^-. In the case of F^-, *n* was <1 in both the binary and the simple systems for most sorbents (except forest soil, which is around 1, and the pyritic material and mussel shell, which is >1) (Table 2). The presence of Cr(VI) does not modify the value of *n* in forest soil, but caused a decrease in vineyard soil, pine bark, hemp waste, and pine sawdust, and caused an increase in pyritic material, mussel shell, and oak ash. These results would indicate that for most of the sorbents, F^- is adsorbed on high energy heterogeneous sites in both binary and simple systems, and the presence of Cr(VI) affects the interaction with sorbate, favoring it in some cases, and hampering it in other, which coincides with experimental data for forest soil, pyritic material, oak ash, and mussel shell, but not for vineyard soil, pine bark, hemp waste, and pine sawdust.

Li et al. [2], and Deng et al. [48], reported increased F^- adsorption in binary as compared to simple systems, while Cr(VI) adsorption decreased. In addition, in the present study, *n* values in the binary system were lower for F^- than for Cr(VI) in most sorbents, with the exception of pyritic material and oak ash, which would indicate that the highest energy sites are occupied by F^- in most materials.

In addition, Table 3 shows the fitting of adsorption data to the Temkin model. This model assumes that adsorption is characterized by uniform binding energies distribution up to the maximum level [58], and that adsorption energy decreases linearly with surface occupation. As shown in Table 3, in some cases error values were too high to allow adjustment. Taking into account that this model is considered appropriate for chemical adsorption based on strong electrostatic interactions, those cases where the model fits well can be considered indicative of the relevance of chemisorption, as previously reported by Gao et al. [59] and by Rajapaksha et al. [60].

Table 3. Parameters of the Temkin model for Cr(VI) and F^- in individual simple (S) and competitive binary (B) systems.

Adsorbent	Adsorbate	Temkin Parameter				
		b_t	Error	K_t (L g^{-1})	Error	R^2
Forest soil	Cr (S)	3,176,374.39	0.485	-	-	0.680
	Cr (B)	813,385.42	1.022	2.361	1.303	0.897
	F (S)	126,626.39	2.385	4.083	0.610	0.983
	F (B)	128,112.72	2.604	4.905	0.853	0.980
Vineyard soil	Cr (S)	780,829.49	1.226	2.075	1.242	0.866
	Cr (B)	1,035,341.41	0.911	2.316	1.458	0.874
	F (S)	280,522.19	1.661	5.973	2.167	0.965
	F (B)	272,680.16	0.924	4.480	0.789	0.989
Pyritic material	Cr (S)	463,270.75	0.727	112.489	60.409	0.983
	Cr (B)	-	-	235.022	170.959	0.974
	F (S)	-	-	4.574	1.657	0.939
	F (B)	325,525.16	3.093	4.189	3.104	0.862

Table 3. *Cont.*

Adsorbent	Adsorbate	Temkin Parameter				
		b_t	Error	K_t (L g^{-1})	Error	R^2
Pine bark	Cr (S)	189,257.65	6.035	222.501	214.420	0.781
	Cr (B)	134,453.35	5.739	120.715	66.304	0.912
	F (S)	207,675.77	1.763	7.664	2.080	0.977
	F (B)	-	-	4.268	1.207	0.982
Hemp waste	Cr (S)	-	-	2.755	2.094	0.824
	Cr (B)	-	-	-	-	-
	F (S)	-	-	-	-	-
	F (B)	-	-	2.430	1.127	0.943
Pine sawdust	Cr (S)	-	-	25.597	29.425	0.464
	Cr (B)	-	-	-	-	-
	F (S)	-	-	-	-	-
	F (B)	-	-	-	-	-
Mussel shell	Cr (S)	-	-	-	-	-
	Cr (B)	-	-	1.144	0.763	0.717
	F (S)	-	-	-	-	-
	F (B)	-	-	2.052	1.302	0.693
Oak ash	Cr (S)	-	-	2.221	0.818	0.935
	Cr (B)	-	-	3.808	0.417	0.996
	F (S)	-	-	15.540	9.444	0.910
	F (B)	-	-	4.866	1.858	0.956

b_t: Temkin isotherm constant; K_t: Tempkin isotherm equilibrium binding constant; R^2: coefficient of determination; -: adjustment not allowed due to high error values.

4. Conclusions

Competitive adsorption was studied for F^- and Cr(VI) in binary systems where the same concentrations of both pollutants were added simultaneously. The pH values of the adsorbent materials used determine their affinity for both pollutants, causing those with higher pH to have a higher affinity for F^-, while lower pH values favor Cr(VI) adsorption. In the soils studied, the simultaneous presence of F^- and Cr(VI) does not modify Cr(VI) adsorption, but decreases that of F^- compared to the simple systems, especially in the vineyard soil. The presence of Cr(VI) also hinders F^- adsorption in all by-products, while F^- decreased Cr(VI) retention in pine sawdust, hemp waste, and mussel shell. When both pollutants are present simultaneously, Cr(VI) occupies the highest energy adsorption sites in both soils, and also in pine bark, while they are occupied by F^- in the other adsorbent materials studied here. In episodes of contamination in which F^- and Cr(VI) are involved simultaneously, the use of only one of the bioadsorbents could be not effective to successfully retain both pollutants. However, the problem could be addressed using mixtures of two bioadsorbents. Specifically, pine bark would adsorb most Cr(VI), and oak ash would perform very effectively in removing F^- from binary systems, which could be of great aid in the case of soils having low adsorption capacity for these two pollutants.

Supplementary Materials: The following are available online at http://www.mdpi.com/2227-9717/7/10/748/s1, Table S1: General characteristics of the sorbent materials (average values for 3 replicates, with coefficients of variation always <5%), Figure S1: Infrared spectrum of forest soil, Figure S2: Infrared spectrum of vineyard soil, Figure S3: Infrared spectrum of pyritic material, Figure S4: Infrared spectrum of fine mussel shell, Figure S5: Infrared spectrum of pine bark, Figure S6: Infrared spectrum of oak ash, Figure S7: Infrared spectrum of hemp waste, Figure S8. Infrared spectrum of pine sawdust, Figure S9: Fitting of Cr(VI) adsorption data to the Freundlich model for simple (S) and binary (B) experiments, Figure S10: Fitting of F^- adsorption data to the Freundlich model for simple (S) and binary (B) experiments.

Author Contributions: Conceptualization, E.Á.-R., M.J.F.-S., and A.N.-D.; methodology, E.Á.-R., M.J.F.-S., and A.N.-D.; software, G.F.-C., M.A.-E., J.C.N.-M., and D.F.-C.; validation, E.Á.-R., M.J.F.-S., A.N.-D., M.A.-E., J.C.N.-M., and D.F.-C.; formal analysis, A.Q.-F.; investigation, A.Q.-F. and G.F.-C.; resources, E.Á.-R. and M.A.-E.; data

curation, E.Á.-R., M.J.F.-S., and A.N.-D.; writing—original draft preparation, A.Q.-F., E.Á.-R., and M.J.F.-S.; writing—review and editing, A.N.-D.; visualization, All authors; supervision, E.Á.-R. and M.A.-E.; project administration, E.Á.-R. and M.A.-E.; funding acquisition, E.Á.-R. and M.A.-E.

Funding: This research was funded by the SPANISH MINISTRY OF ECONOMY AND COMPETITIVENESS by means of the research projects CGL2012-36805-C02-01 and CGL2012-36805-C02-02. It was also partially financed by the European Regional Development Fund (FEDER in Spain). The APC was not funded but waived by MDPI.

Conflicts of Interest: The authors declare no conflict of interest.

References

1. Aoudj, S.; Khelifa, A.; Drouiche, N.; Belkada, R.; Miroud, D. Simultaneous removal of chromium(VI) and fluoride by electrocoagulation–electroflotation: Application of a hybrid Fe-Al anode. *Chem. Eng. J.* **2015**, *267*, 153–162. [CrossRef]
2. Li, T.; Xie, D.; He, C.; Xu, X.; Huang, B.; Nie, R.; Liu, S.; Duan, Z.; Liu, W. Simultaneous adsorption of fluoride and hexavalent chromium by synthetic mesoporous alumina: Performance and interaction mechanism. *RSC Adv.* **2016**, *6*, 48610–48619. [CrossRef]
3. Rafique, T.; Naseem, S.; Bhanger, M.I.; Usmani, T.H. Fluoride ion contamination in the groundwater of Mithi sub-district, the Thar Desert, Pakistan. *Environ. Geol.* **2008**, *56*, 317–326. [CrossRef]
4. Kumar, A.; Parimal, P.; Nataraj, S.K. Bionanomaterial scaffolds for effective removal of fluoride, chromium, and dye. *ACS Sustain. Chem. Eng.* **2016**, *5*, 895–903. [CrossRef]
5. Wang, Y.; Reardon, E.J. Activation and regeneration of a soil sorbent for defluoridation of drinking water. *Appl. Geochem.* **2001**, *16*, 531–539. [CrossRef]
6. Li, L.; Li, Y.X.; Cao, L.X.; Yang, C.F. Enhanced chromium (VI) adsorption using nanosized chitosan fibers tailored by electrospinning. *Carbohydr. Polym.* **2015**, *125*, 206–213. [CrossRef] [PubMed]
7. Alvarez-Ayuso, E.; Garcia-Sanchez, A.; Querol, X. Adsorption of Cr(VI) from synthetic solutions and electroplating wastewaters on amorphous aluminium oxide. *J. Hazard. Mater.* **2007**, *142*, 191–198. [CrossRef]
8. Teng, S.X.; Wang, S.G.; Gong, W.X.; Liu, X.W.; Gao, B.Y. Removal of fluoride by hydrous manganese oxide-coated alumina: Performance and mechanism. *J. Hazard. Mater.* **2009**, *168*, 1004–1011. [CrossRef]
9. Mohapatra, M.; Anand, S.; Mishra, B.K.; Giles, D.E.; Singh, P. Review of fluoride removal from drinking water. *J. Environ. Manag.* **2009**, *91*, 67–77. [CrossRef]
10. Gago, C.; Romar, A.; Fernández-Marcos, M.L.; Álvarez, E. Fluorine sorption by soils developed from various parent materials in Galicia (NW Spain). *J. Colloid Interface Sci.* **2012**, *374*, 232–236. [CrossRef]
11. Quintáns-Fondo, A.; Ferreira-Coelho, G.; Paradelo-Núñez, R.; Nóvoa-Muñoz, J.C.; Arias-Estévez, M.; Fernández-Sanjurjo, M.J.; Álvarez-Rodríguez, E.; Núñez-Delgado, A. F sorption/desorption on two soils and on different by-products and waste materials. *Environ. Sci. Pollut. Res.* **2016**, *23*, 14676–14685. [CrossRef] [PubMed]
12. Quintáns-Fondo, A.; Santás-Miguel, V.; Nóvoa-Muñoz, J.C.; Arias-Estévez, M.; Fernández-Sanjurjo, M.J.; Álvarez-Rodríguez, E.; Núñez-Delgado, A. Effects of changing pH, incubation time, and As(V) competition, on F−retention on soils, natural adsorbents, by-products, and waste materials. *Front. Chem.* **2018**, *6*, 51–60. [CrossRef] [PubMed]
13. Romar-Gasalla, A.; Santás-Miguel, V.; Nóvoa-Muñoz, J.C.; Arias-Estévez, M.; Álvarez-Rodríguez, E.; Núñez-Delgado, A.; Fernández-Sanjurjo, M.J. Chromium and fluoride sorption/desorption on un-amended and waste amended forest and vineyard soils and pyritic material. *J. Environ. Manag.* **2018**, *222*, 3–11. [CrossRef] [PubMed]
14. Alejano, L.R.; Perucho, A.; Olalla, C.; Jiménez, R. *Rock Engineering and Rock Mechanics: Structures in and on Rock Masses*; CRC Press: London, UK, 2014; p. 372.
15. Álvarez, E.; Fernández-Sanjurjo, M.J.; Núñez, A.; Seco, N.; Corti, G. Aluminium fractionation and speciation in bulk and rhizosphere of a grass soil amended with mussel shells or lime. *Geoderma* **2012**, *173–174*, 322–329. [CrossRef]
16. Banerjee, S.; Chattopadhyaya, M.C. Adsorption characteristics for the removal of a toxic dye, tartrazine from aqueous solutions by a low cost agricultural by-product. *Arab. J. Chem.* **2017**, *10*, S1629–S1638. [CrossRef]
17. Brás, I.; Teixeira-Lemos, L.; Alves, A.; Pereira, M.F.R. Application of pine bark as a sorbent for organic pollutants in effluents. *Manag. Environ. Qual. Int. J.* **2004**, *15*, 491–501. [CrossRef]

18. Chatterjee, A.; Lal, R.; Wielopolski, L.; Martin, M.Z.; Ebinger, M.H. Evaluation of different soil carbon determination methods. *Crit. Rev. Plant Sci.* **2009**, *28*, 164–178. [CrossRef]
19. Coelho, G.F.; ConÇalves, A.C.; Tarley, C.R.T.; Casarin, J.; Nacke, N.; Francziskowski, M.A. Removal of metal ions Cd (II), Pb (II) and Cr (III) from water by the cashew nut shell *Anarcadium occidentale* L. *Ecol. Eng.* **2014**, *73*, 514–525. [CrossRef]
20. Dlapa, P.; Bodí, M.B.; Mataix-Solera, J.; Cerdà, A.; Doerr, S.H. FT-IR spectroscopy reveals that ash water repellency is highly dependent on ash chemical composition. *Catena* **2013**, *108*, 35–43. [CrossRef]
21. Fackler, K.; Stevanic, J.S.; Ters, T.; Hinterstoisser, B.; Schwanninger, M.; Salmén, L. Localisation and characterisation of incipient brown-rot decay within spruce wood cell walls using FT-IR imaging microscopy. *Enzym. Microb. Technol.* **2010**, *47*, 257–267. [CrossRef]
22. Haberhauer, G.; Gerzabek, M.H. Drift and transmission FT-IR spectroscopy of forest soils: An approach to determine decomposition processes of forest litter. *Vib. Spectrosc.* **1999**, *19*, 413–417. [CrossRef]
23. Kamprath, E.J. Exchangeable aluminium as a criterion for liming leached mineral soils. *Soil Sci. Soc. Am. Proc.* **1970**, *34*, 252–254. [CrossRef]
24. Margenot, A.J.; Calderón, F.J.; Goyne, K.W.; Mukome, F.N.D.; Parikh, S.J. IR spectroscopy, soil analysis applications. In *Encyclopedia of Spectroscopy and Spectrometry*, 3rd ed.; Lindon, J., George, E., Tranter, D.K., Eds.; Academic Press: Cambridge, MA, USA, 2017; Volume 2, pp. 448–454. [CrossRef]
25. McLean, E.O. Soil pH and lime requirement. In *Methods of Soil Analysis, Part 2, Chemical and Microbiological Properties*, 2nd ed.; Page, A.L., Miller, R.H., Keeney, D.R., Eds.; ASA: Madison, WI, USA, 1982; Volume 2, pp. 199–223.
26. Mimura, A.M.S.; Vieira, T.V.A.; Martinelli, P.B.; Gorgulho, H.F. Utilization of rice husk to remove Cu^{2+}, Al^{3+}, Ni^{2+} and Zn^{2+} from wastewater. *Química Nova* **2010**, *33*, 1279–1284. [CrossRef]
27. Movasaghi, Z.; Rehman, S.; Rehman, I. Fourier transform infrared (FTIR) spectroscopy of biological tissues. *Appl. Spectrosc. Rev.* **2008**, *43*, 134–179. [CrossRef]
28. Nóbrega, J.A.; Pirola, C.; Fialho, L.L.; Rota, G.; de Campos, C.E.; Pollo, F. Microwave-assisted digestion of organic samples: How simple can it become? *Talanta* **2012**, *98*, 272–276. [CrossRef]
29. Pavia, D.L.; Lampman, G.M.; Kriz, G.S.; Vyvyan, J.R. *Introdução à Espectroscopia*, 4th ed.; Cengage Learning: São Paulo, Bresil, 2010; p. 700.
30. Rubio, F.; GonÇalves, A.C., Jr.; Meneghel, A.P.; Tarley, C.R.T.; Schwantes, D.; Coelho, G.F. Removal of cadmium from water using by-product *Crambe abyssinica* Hochst seeds as biosorbent material. *Water Sci. Technol.* **2013**, *68*, 227–233. [CrossRef]
31. Saikia, B.J.; Parthasarathy, G. Fourier transform infrared spectroscopic characterization of kaolinite from Assam and Meghalaya, Northeastern India. *J. Mod. Phys.* **2010**, *1*, 206–210. [CrossRef]
32. Sila, A.M.; Shepherd, K.D.; Pokhariyal, G.P. Evaluating the utility of mid-infrared spectral subspaces for predicting soil properties. *Chemom. Intell. Lab. Syst.* **2016**, *153*, 92–105. [CrossRef]
33. Smidt, W.; Meissl, K. The applicability of Fourier transform infrared (FT-IR) spectroscopy in waste management. *Waste Manag.* **2007**, *27*, 268–276. [CrossRef]
34. Sumner, M.E.; Miller, W.P. Cation exchange capacity and exchange coefficients. In *Methods of Soil Analysis, Part 3, Chemical Methods*; Bartels, J.M., Bigham, J.M., Eds.; ASA: Madison, WI, USA, 1996; Volume 3, pp. 437–474.
35. Tan, K.H. *Soil Sampling, Preparation, and Analysis*; Marcel Dekker: New York, NY, USA, 1996; p. 408.
36. Tarley, C.R.T.; Arruda, M.A.Z. Biosorption of heavy metals using rice milling by-products. Characterisation and application for removal of metals from aqueous effluents. *Chemosphere* **2004**, *54*, 987–995. [CrossRef]
37. Tinti, A.; Tugnoli, V.; Bonora, S.; Francioso, O. Recent applications of vibrational mid-Infrared (IR) spectroscopy for studying soil components: A review. *J. Cent. Eur. Agric.* **2015**, *16*. [CrossRef]
38. Mahapatra, A.; Mishra, B.G.; Hota, G. Studies on Electrospun Alumina Nanofibers for the Removal of Chromium(VI) and Fluoride Toxic Ions from an Aqueous System. *Ind. Eng. Chem. Res.* **2013**, *52*, 1554–1561. [CrossRef]
39. Wang, X.S.; Li, Z.Z.; Tao, S.R. Removal of chromium (VI) from aqueous solution using walnut hull. *J. Environ. Manag.* **2009**, *90*, 721–729. [CrossRef] [PubMed]
40. Choppala, G.; Bolan, N.; Lamb, D.; Kunhikrishnan, A. Comparative sorption and mobility of Cr(III) and Cr(VI) species in a range of soils: Implications to bioavailability. *Water Air Soil Pollut.* **2013**, *224*, 1699–1711. [CrossRef]

41. Griffin, R.; Au, A.K.; Frost, R. Effect of pH on adsorption of chromium from landfill-leachate by clay minerals. *J. Environ. Sci. Health A* **1977**, *12*, 431–449. [CrossRef]
42. Cutillas-Barreiro, L.; Ansias-Manso, L.; Calviño, D.F.; Arias-Estévez, M.; Nóvoa-Muñoz, J.C.; Fernández-Sanjurjo, M.J.; Álvarez-Rodríguez, E.; Núñez-Delgado, A. Pine bark as bio-adsorbent for Cd, Cu, Ni, Pb and Zn: Batch-type and stirred flow chamber experiments. *J. Environ. Manag.* **2014**, *144*, 258–264. [CrossRef]
43. Paradelo, R.; Cutillas-Barreiro, L.; Soto-Gomez, D.; Novoa-Muñoz, J.C.; Arias-Estevez, M.; Fernández-Sanjurjo, M.J.; Álvarez-Rodríguez, E.; Núñez-Delgado, A. Study of metal transport through pine bark for reutilization as a biosorbent. *Chemosphere* **2016**, *149*, 146–153. [CrossRef]
44. Fernández-Pazos, M.T.; Garrido-Rodriguez, B.; Nóvoa-Muñoz, J.C.; Arias-Estévez, M.; Fernández-Sanjurjo, M.J.; Núñez-Delgado, A.; Álvarez, E. Cr(VI) adsorption and desorption on soils and biosorbents. *Water Air Soil Pollut.* **2013**, *224*, 1366. [CrossRef]
45. Otero, M.; Cutillas-Barreiro, L.; Nóvoa-Muñoz, J.C.; Arias-Estévez, M.; Álvarez-Rodríguez, E.; Fernández-Sanjurjo, M.J.; Núñez-Delgado, A. Cr(VI) sorption/desorption on untreated and mussel-shell-treated soil materials: Fractionation and effects of pH and chromium concentration. *Solid Earth* **2015**, *6*, 373–382. [CrossRef]
46. Gago, C.; Romar, A.; Fernández-Marcos, M.L.; Álvarez, E. Fluorine sorption and desorption on soils located in the surroundings of an aluminium smelter in Galicia (NW Spain). *Environ. Earth Sci.* **2014**, *72*, 4105–4114. [CrossRef]
47. Alexandratos, V.G.; Elzinga, E.J.; Reeder, R.J. Arsenate uptake by calcite: Macroscopic and spectroscopic characterization of adsorption and incorporation mechanisms. *Geochim. Cosmochim. Acta* **2007**, *71*, 4172–4187. [CrossRef]
48. Deng, H.; Yu, X. Adsorption of fluoride, arsenate and phosphate in aqueous solution by cerium impregnated fibrous protein. *Chem. Eng. J.* **2012**, *184*, 205–212. [CrossRef]
49. Wu, Y.; Ma, X.; Feng, M.; Liu, M. Behavior of chromium and arsenic on activated carbon. *J. Hazard. Mater.* **2008**, *159*, 380–384. [CrossRef] [PubMed]
50. Liu, W.; Wnag, T.; Borthwick, A.; Wang, Y.; Yin, X.; Li, X.; Ni, J. Adsorption of Pb^{2+}, Cd^{2+}, Cu^{2+} and Cr^{3+} onto titanate nanotubes: Competition and effect of inorganic ions. *Sci. Total Environ.* **2013**, *456–457*, 171–180. [CrossRef]
51. Ucun, H.; Bayhan, Y.K.; Kaya, Y.; Cakici, A.; Algur, O.F. Biosorption of chromium (VI) form aqueous solution by cone biomass of *Pinus sylvestris*. *Bioresource Technol.* **2002**, *85*, 155–158. [CrossRef]
52. Núñez-Delgado, A.; Fernández-Sanjurjo, M.J.; Álvarez-Rodríguez, E.; Cutillas-Barreiro, L.; Nóvoa-Muñoz, J.C.; Arias-Estévez, M. Cr(VI) sorption/desorption on pine sawdust and oak wood ash. *Int. J. Environ. Res. Public Health* **2015**, *12*, 8849–8860. [CrossRef]
53. Khezami, L.; Capart, R. Removal of chromium (VI) from aqueous solution by activated carbons: Kinetic and equilibrium studies. *J. Hazard. Mater.* **2005**, *123*, 223–231. [CrossRef]
54. Bhaumik, R.; Mondal, N.K.; Das, B.; Roy, P.K.C. Eggshell powder as an adsorbent for removal of fluoride from aqueous solution: Equilibrium, kinetic and thermodynamic studies. *J. Chem.* **2012**, *9*, 1457–1480. [CrossRef]
55. Vijayaraghavan, K.; Palanivelu, K.; Velan, M. Biosorption of copper(II) and cobalt(II) from aqueous solutions by crab shell particles. *Bioresour. Technol.* **2006**, *97*, 1411–1419. [CrossRef]
56. Behnajady, M.A.; Bimeghdar, S. Synthesis of mesoporous NiO nanoparticles and their application in the adsorption of Cr(VI). *Chem. Eng. J.* **2014**, *239*, 105–113. [CrossRef]
57. Foo, K.Y.; Hameed, B.H. Insights into the modeling of adsorption isotherm systems. *Chem. Eng. J.* **2010**, *156*, 2–10. [CrossRef]
58. Ofomaja, A.E.; Unuabonah, E.I. Kinetics and time-dependent Langmuir modeling of 4-nitrophenoladsorption onto *Mansonia* sawdust. *J. Taiwan Inst. Chem. Eng.* **2013**, *44*, 566–567. [CrossRef]

59. Gao, Y.; Li, Y.; Zhang, L.; Huang, H.; Hu, J.; Shah, S.M.; Su, X. Adsorption and removal of tetracycline antibiotics from aqueous solution by graphene oxide. *J. Colloid Interface Sci.* **2012**, *368*, 540–546. [CrossRef] [PubMed]
60. Rajapaksha, A.U.; Vithanage, M.; Ahmad, M.; Seo, D.C.; Cho, J.S.; Lee, S.E.; Ok, Y.S. Enhanced sulfamethazine removal by steam-activated invasive plant-derived biochar. *J. Hazard. Mater.* **2015**, *290*, 43–50. [CrossRef]